European Radiology (2023) 33:6001–6008
https://doi.org/10.1007/s00330-023-09599-9

European Radiology
EUROPEAN SOCIETY OF RADIOLOGY

MAGNETIC RESONANCE

Correlation of R2* with fat fraction and bone mineral density and its role in quantitative assessment of osteoporosis

Zhenghua Liu[1] · Dageng Huang[2] · Yonghong Jiang[1] · Xiaowen Ma[1] · Yuting Zhang[1] · Rong Chang[1]

Received: 7 October 2022 / Revised: 2 February 2023 / Accepted: 22 February 2023 / Published online: 5 April 2023

Abstract

Objectives To investigate the correlation of R2* with vertebral fat fraction (FF) and bone mineral density (BMD), and to explore its role in the quantitative assessment of osteoporosis (OP).

Methods A total of 83 patients with low back pain (59.77 ± 7.46 years, 30 males) were enrolled, which underwent lumbar MRI in IDEAL-IQ sequences and quantitative computed tomography (QCT) scanning within 48h. The FF, R2*, and BMD of all 415 lumbar vertebrae were respectively measured. According to BMD, all vertebrae were divided into BMD normal, osteopenia, and OP groups, and the difference of FF and R2* among groups was analyzed by one-way ANOVA. The correlation between R2*, FF, and BMD was analyzed by Pearson's test. Taking BMD as the gold standard, the efficacies for FF and R2* in diagnosis of OP and osteopenia were assessed by receiver operating characteristic curve, and their area under the curve (AUC) was compared with DeLong's test.

Results The FF and R2* were statistically different among groups (F values of 102.521 and 11.323, both $p < 0.05$), and R2* were significantly correlated with FF and BMD, respectively (r values of −0.219 and 0.290, both $p < 0.05$). In diagnosis of OP and osteopenia, the AUCs were 0.776 and 0.778 for FF and 0.638 and 0.560 for R2*, and the AUCs of R2* were lower than those of FF, with Z values of 4.030 and 4.087, both $p < 0.001$.

Conclusion R2* is significantly correlated with FF and BMD and can be used as a complement to FF and BMD for quantitative assessment of OP.

Key Points

- *R2* based on IDEAL-IQ sequences has a definite but weak linear relationship with FF and BMD.*
- *FF is significantly correlated with BMD and can effectively evaluate BMAT.*
- *R2* can be used as a complement to FF and BMD for fine quantification of bone mineral loss and bone marrow fat conversion.*

Keywords Magnetic resonance imaging · Bone density · Osteoporosis · Bone marrow · Adipose tissue

Abbreviations

AUC	Area under the curve
BMAT	Bone marrow adipose tissue
BMD	Bone mineral density
FF	Fat fraction
ICC	Intraclass correlation coefficient
IDEAL-IQ	Iterative decomposition of water and fat with echo asymmetry and least-squares estimation
MRI	Magnetic resonance imaging
OP	Osteoporosis
QCT	Quantitative computed tomography
ROC	Receiver operating characteristic
ROI	Region of interest

✉ Yonghong Jiang
526017009@qq.com

✉ Xiaowen Ma
14125572@qq.com

[1] Department of Radiology, Honghui Hospital Affiliated Xi'an Jiaotong University, No. 555, Youyi East Road, Xi'an 710054, China

[2] Department of Spinal Surgery, Honghui Hospital Affiliated Xi'an Jiaotong University, No. 555, Youyi East Road, Xi'an 710054, China

Introduction

Osteoporosis (OP) is an age-increasing disease that seriously affects the health of the elderly, and its diagnosis and evaluation rely mainly on bone mineral density (BMD) measurements [1, 2]. Recent studies have shown that bone marrow

adipose tissue (BMAT) plays an important role in the development and progression of osteoporosis (OP), and may be a biomarker for OP [3–5]. Further studies have pointed out that differences in BMAT amounts may reduce the accuracy of BMD and that BMAT should be quantified to correct for BMD [6, 7].

Magnetic resonance imaging (MRI) has clear advantages in quantifying bone marrow composition [8], such as iterative decomposition of water and fat with echo asymmetry and least-squares estimation quantitation (IDEAL-IQ) sequences [9, 10]; based on multi echo acquisition, it can obtain fat fraction (FF) imaging, R2* imaging, fat imaging, and water imaging through one scan [11]. In Ergen's study [12], a significant negative correlation was found between FF and BMD of the vertebral body, suggesting that loss of vertebral bone mineral can be assessed using FF. In Ji's study [13], FF and R2* were used to quantify the vertebral BMAT and found that the BMAT was associated with degeneration of the adjacent discs.

R2*, the inverse of the effective transverse relaxation time [T2*], is a derived research product that has received increasing attention in recent studies. In the spine, R2* has been tried for the differentiation of osteoporotic, traumatic, and malignant vertebral fractures [14–16] and also to distinguish aplastic anemia from myelodysplastic syndromes [17]. Some other studies have pointed out that R2* (T2*) of the vertebral bone marrow correlates with the ferritin content of the red bone marrow as well as the density and orientation of the trabeculae [18, 19].

We were interested in the correlation between R2* and BMAT content of the vertebral body as well as BMD. However, the relationship between R2* with FF and BMD has been rarely reported and remains controversial [18, 20, 21], and its role in the quantitative assessment of OP still needs further validation. In this study, we enrolled a group of patients with chronic low back pain who underwent IDEAL-IQ sequences scan of the lumbar spine as well as QCT scan, and we aimed to investigate the correlation between R2* with FF and BMD, and to explore its role in the quantitative assessment of OP.

Materials and methods

Study design

The present study was conducted following the Declaration of Helsinki (as revised in 2013) and approved by the Ethics Committee of our hospital (IRB No. 201902068). This is a secondary analysis of a prospective study, and some patients with chronic low back pain received MRI and QCT scans at the recommendation of surgeons and were initially included in the study. Inclusion criteria were as follows: (1) age should be ≥ 50 years; (2) lumbar MRI and QCT scan within 48 h. Exclusion criteria included the following points: (1) scoliosis; (2) localized osteosclerosis in vertebral cancellous bone; (3) vertebral trauma and tumor; (4) metabolic and hematopoietic system diseases other than osteoporosis; (5) postoperative state of lumbar vertebra. The flowchart displaying patient inclusion of this study is shown in Fig. 1.

MRI scanning

MRI examinations relied on a 3.0-T superconducting MR scanner (Discovery 750, GE Healthcare), with standard human body coil and sagittal scanning. Prior to IDEAL-IQ, T1-weighted image (T1WI) (repetition time (TR)/time to echo (TE) = 400/13 ms), T2WI (TR/TE = 2500/102 ms), FOV 36 cm ×36 cm, matrix of 224 × 192, pixel size 1.6 mm × 1.9 mm, slice thickness of 3 mm, intersection gap of 0.4, number of excitations (NEX) of 1; IDEAL-IQ: TR of 7.4 ms, minimum TE of 1.3 ms, maximum TE of 5.3 ms, flip angle of 4°, echo train length of 5, bandwidth of 111.1 kHz, and other settings were the same as above. Four group images were acquired in once scanning with IDEAL-IQ sequence: pure water image, pure fat image, fat fraction image, and R2* relaxation rate image.

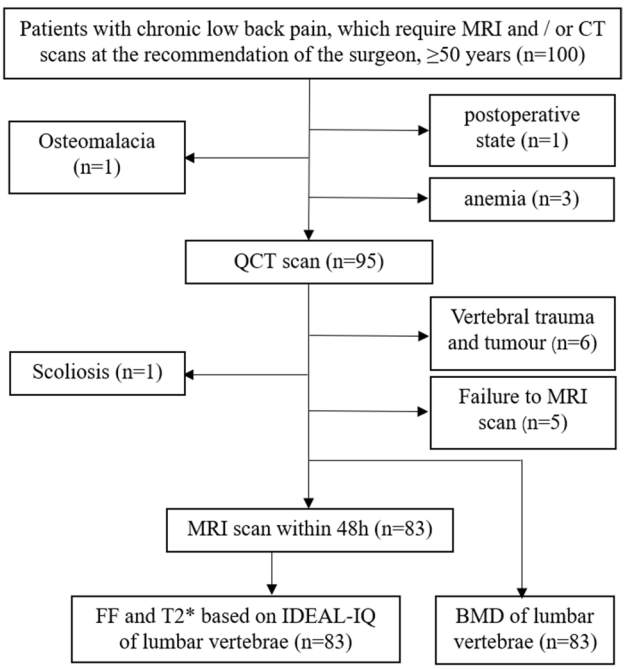

Fig. 1 The flowchart of the study. CT, computed tomography; QCT, quantitative computed tomography; MRI, magnetic resonance imaging; FF, fat fraction; BMD, bone mineral density

Image analysis

The measurement of FF and R2* was performed on the viewer module of ADW 4.7 workstation. Select the FF image and R2* relaxation rate image respectively, draw a rectangular region of interest (ROI) on the first 2/3 of the vertebral body in the median sagittal diagram, avoiding the vertebral vein sulcus; then, the FF and R2* values of 1st to 5th lumbar vertebrae were measured successively at one slice (Fig. 2a, b). All vertebral measurements were performed independently by two doctors with more than 8 years of experience in musculoskeletal radiology, and take the mean value of 2 measurers as the final value.

QCT-based BMD measurement and grouping

CT equipment (Somatom Definition Flash; Siemens Healthineers) and QCT analytics (QCT Pro v5.0; Mindways) were calibrated in advance using a quality control phantom. Constant X-ray tube and reconstruction parameter setting were used. A standard QCT corrected phantom was placed under the waist during CT procedure, and the scan data was imported to the QCT analytics. The system generated ROIs in the cancellous bone region of the vertebrae, and the BMD values of the 1st to 5th lumbar vertebrae were measured in sequence (Fig. 2c). According to the BMD values, all vertebrae were divided into BMD normal group (BMD >120 mg/cm^3), osteopenia group (120 mg/cm^3 ≥ BMD > 80 mg/cm^3), and OP group (BMD ≤ 80 mg/cm^3) [22].

Statistical analysis

All computations were powered by MedCalc (version 19.0, MedCalc Software) and expressed as the mean ± standard deviation. Consistency analyses for the measurements of the two readers were performed using the intraclass correlation coefficient (ICC) (ICC of < 0.4 means poor consistency, ICC of 0.4~0.75 means general consistency, ICC of > 0.75 means good consistency). Variables were tested for normality of distribution using the Shapiro-Wilk test. Differences between groups were determined using one-way ANOVA and Tukey-Kramer's test. Pearson's test was used to determine the correlation between FF, R2*, and BMD. Taking BMD as the gold standard, the efficacies of FF and R2* for the diagnosis of OP and osteopenia were assessed by receiver operating characteristic (ROC) curve, and their area under the curve (AUC) was compared with DeLong' test. The significance for all tests was set at p value < 0.05.

Results

General information

A total of 83 patients were enrolled in this study. Of them, 30 were males and 53 were females, aged from 50 to 88 years, with an average age of 59.77 ± 7.46 years. The FF and R2* values of all 415 lumbar vertebrae in 83 patients were measured by two doctors, which were in good agreement (ICC = 0.917, 0.886, respectively). The corresponding Bland-Altman plots are shown in Fig. 3, which indicate a reliable agreement between them.

Grouping

All 415 vertebrae were divided into three groups according to BMD. The BMD, FF, and R2* values for each group are shown in Table 1. One-way ANOVA revealed that the overall differences were statistically significant in FF and R2* among groups (F values of 102.521 and 11.323, both $p < 0.05$). The Tukey-Kramer test showed that the pairwise comparison between groups was also statistically significant, respectively, and the multiple comparisons of them are shown in Fig. 4.

Correlation analyses

Pearson's test showed a significant correlation between FF and BMD ($r = -0.624$, $p < 0.001$), and there were also weak correlations between R2* and FF and BMD with r values of 0.219 and 0.290, respectively, both $p < 0.001$ (Fig. 5).

Diagnostic test

The ROC curves for FF and R2* in the diagnosis of OP and osteopenia are shown in Fig. 6, and the threshold, sensitivity, specificity, AUC, and predictive value are shown in Table 2. The DeLong test showed lower AUCs for R2* than for FF in the diagnosis of OP and osteopenia, with Z values of 4.030 and 4.087, respectively, both $p < 0.001$.

Discussion

In this study, we investigated the relationship between vertebral R2* and FF based on MRI in IDEAL-IQ sequence and BMD based on QCT, and then performed diagnostic experiments. The results revealed a definite but weak linear relationship between R2* with FF and BMD, which has limited value

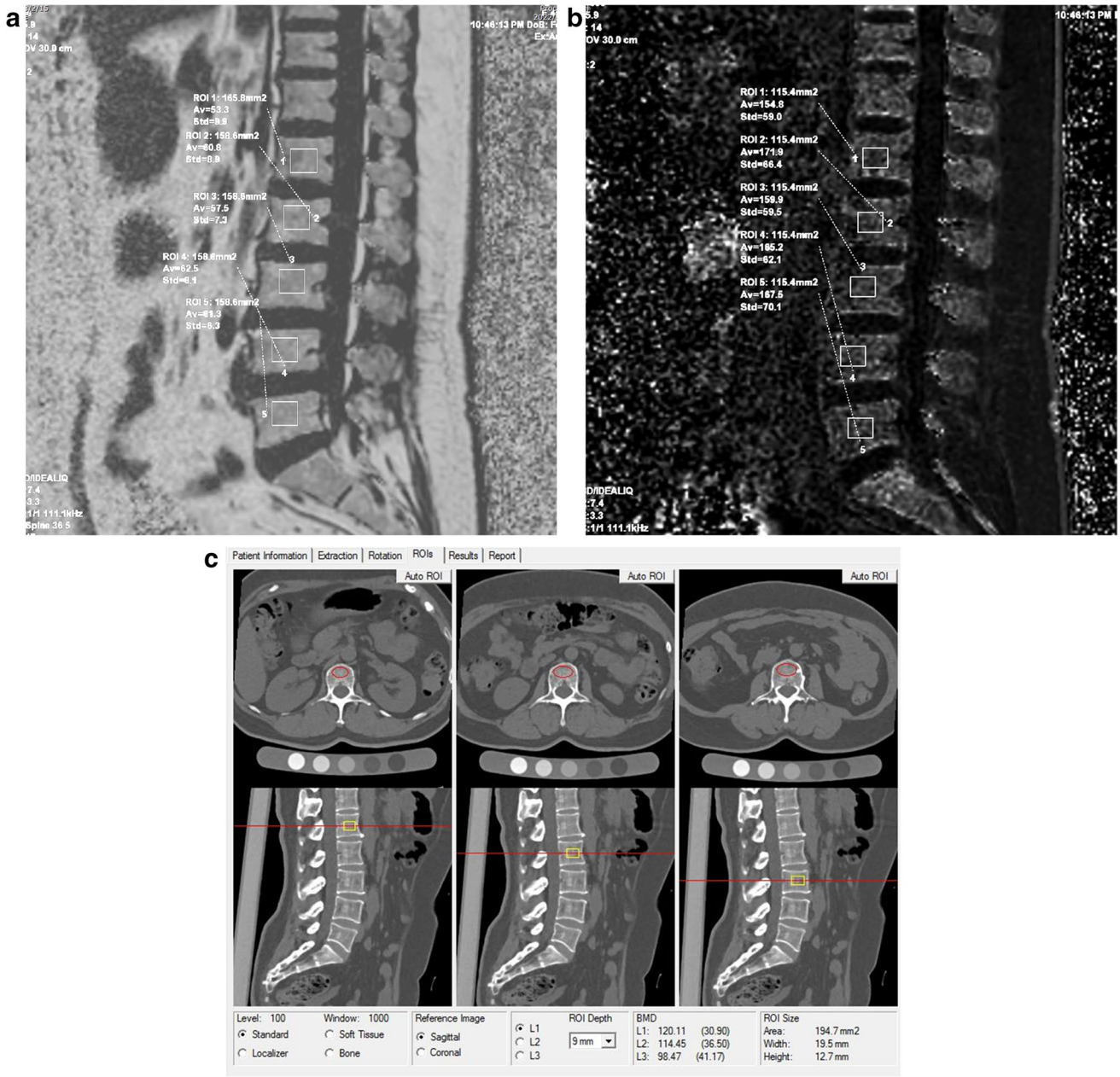

Fig. 2 Measurement of FF, R2*, and BMD. **a** FF image of IDEAL-IQ. **b** R2* relaxation rate image of IDEAL-IQ. **c** Measurement of QCT-based BMD

as a diagnostic indicator for OP and osteopenia, but has some potential as a complement to FF and BMD for fine quantification of bone marrow conversion and bone mineral loss.

Bone marrow is a dynamic organ whose composition changes during growth, aging, and multiple disease processes [23]. During childhood, the bone marrow of the vertebral body consists mainly of red marrow, and as the body ages, BMAT accounts for 70% of the bone marrow due to the conversion of most of the red marrow to yellow marrow [24]. It was noted that BMAT has multiple endocrine effects that inhibit osteoblast differentiation and proliferation, leading to decreased bone formation and reduced BMD [23, 25]. This was confirmed in the present study, where FF of the vertebral body showed a significant negative correlation with BMD, and was of value in the diagnosis of OP, similar to what was previously reported [12].

R2* is associated with the deposition of ferritin in the bone marrow, which is located mainly in the red bone

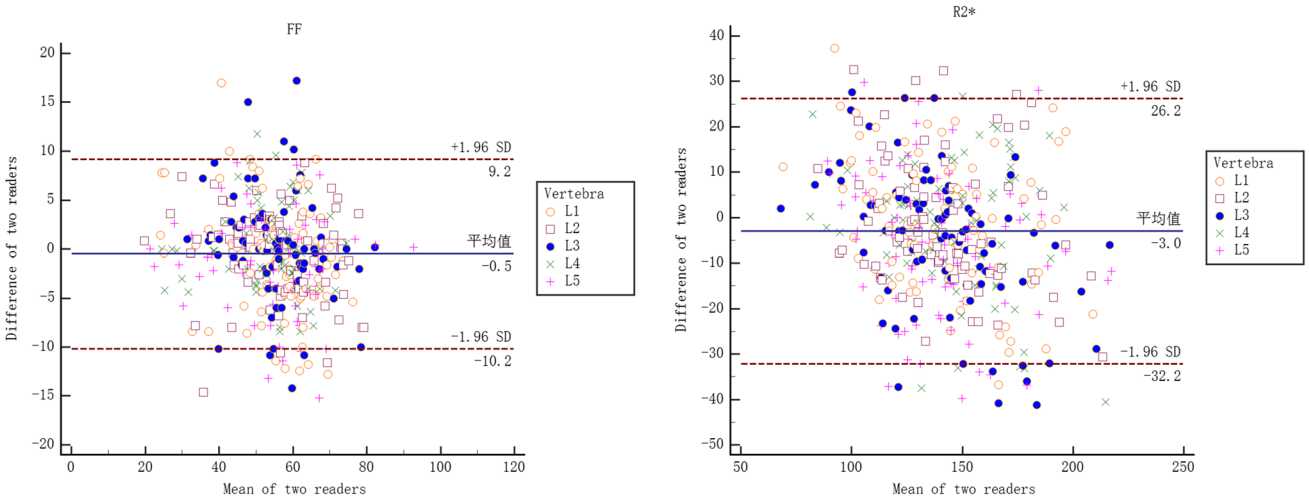

Fig. 3 Bland-Altman plots of two readers for FF and R2* values

Table 1 Measurements of vertebrae in different OP groups ($n = 415$)

	Normal (85)	Osteopenia (164)	OP (166)	Total (415)	*F*	*p*
BMD (mg/cm^3)	141.06 ± 21.62	98.76 ± 11.44	57.68 ± 16.35	90.99 ± 35.16	801.285	< 0.001
FF (%)	43.06 ± 12.18	54.89 ± 8.45	61.13 ± 8.80	54.96 ± 81.55	102.521	< 0.001
R2* (Hz)	149.71 ± 33.87	145.06 ± 24.95	134.34 ± 24.44	141.72 ± 2 7.48	11.323	< 0.001

OP osteoporosis, *BMD* bone mineral density, *FF* fat fraction

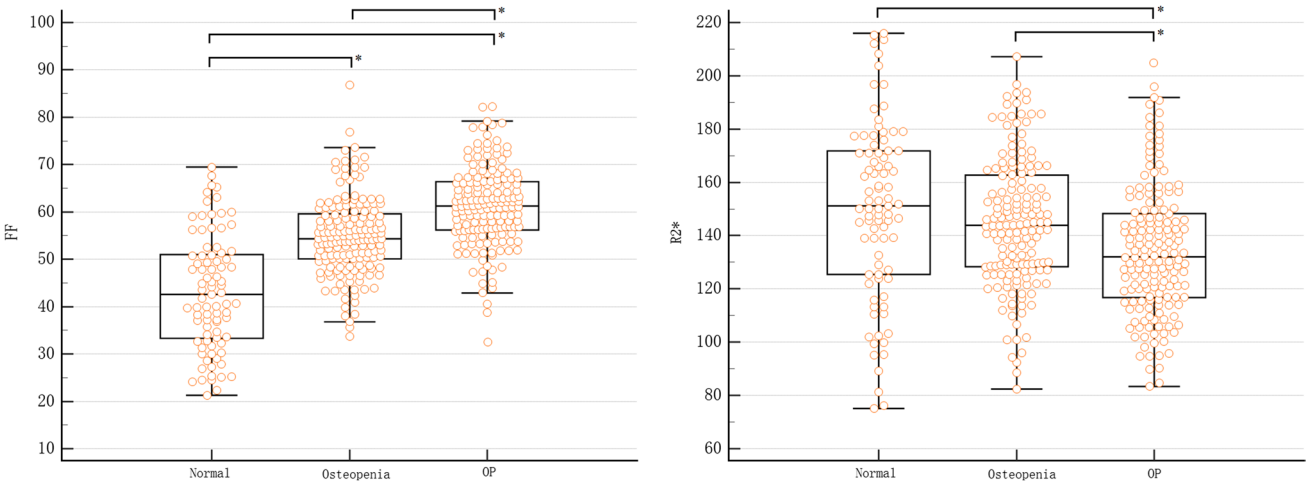

Fig. 4 Comparative plots of FF and R2* for groups. *$p < 0.05$

marrow [17, 18]. In patients with osteoporosis, the bone mineral content is reduced, the bone trabeculae are thinner, the trabecular space is enlarged, its residual space is filled by a large amount of adipose tissue, and the red bone marrow content is relatively reduced, so R2* correlates with both FF and BMD. In addition, it has been shown that bone is more paramagnetic than bone marrow and that the trabecular-bone marrow interface causes local magnetic field inhomogeneity, which can be measured as T2* (R2*) [19]. In the present study, R2* values of vertebrae were positively correlated with BMD and negatively correlated with FF, which we suggest is related to the widening of the trabecular gap, the reduction of the trabecular-marrow interface, and the fatty conversion of red bone marrow when osteoporosis occurs.

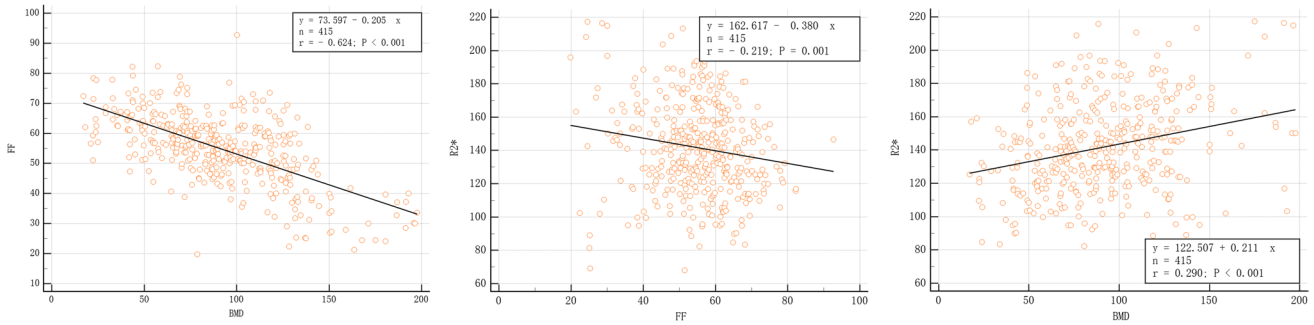

Fig. 5 Correlation between R2*, FF, and BMD

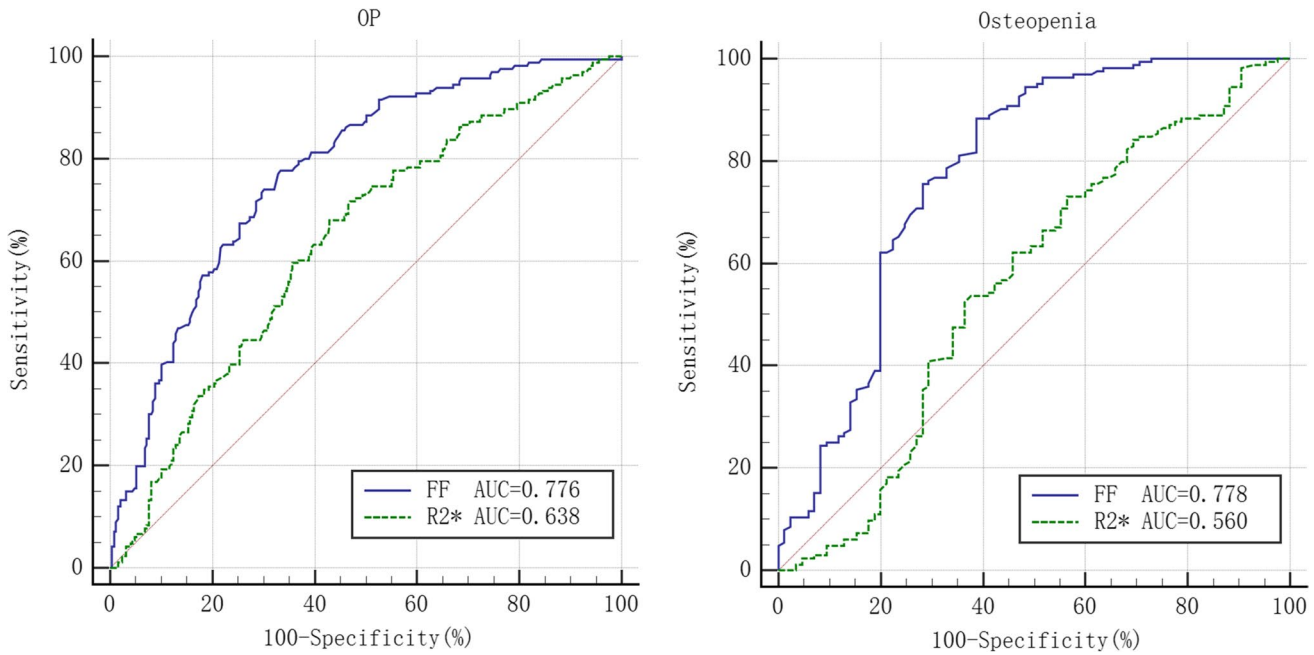

Fig. 6 Efficacy for FF and R2* in OP and osteopenia diagnosis

Table 2 Efficacy for FF and R2* in diagnosis of OP and osteopenia ($n = 415$)

		Threshold	Sensitivity	Specificity	AUC (95%*CI*)	+ PV (%)	- PV (%)
OP	FF (%)	> 55.80	77.71	66.67	0.776 (0.732–0.815)	60.85	81.77
	R2* (Hz)	≤ 142.40	68.07	57.03	0.638 (0.589–0.684)	51.36	72.82
Osteopenia	FF (%)	> 46.30	88.41	61.18	0.778 (0.721–0.828)	60.29	88.79
	R2* (Hz)	≤ 157.70	73.17	53.53	0.560 (0.496–0.623)	51.21	74.95

FF fat fraction, *OP* osteoporosis, AUC area under the curve, + *PV* positive predictive value, - *PV* negative predictive value

Notably, R2* was weakly correlated with FF and BMD, and FF and BMD were significantly correlated in our study, unlike Watanabe's study [21], where R2* was correlated with BMD ($r = 0.602$), but FF was not. We believe that the susceptibility of bone mineral loss and bone marrow fat conversion to other factors (e.g., nutritional fluctuations, hormonal changes, and metabolic disorders) [26] contribute to the different findings. The exclusion of metabolic and hematopoietic system diseases other than osteoporosis in our study and the use of point-to-point ROIs in the data measurements reduced the influence of the above-mentioned factors on

our findings. In the diagnostic test, the AUC of R2* for both diagnosing OP and osteopenia was not high and lower than that of FF in diagnosing OP, which hardly allowed us to use it as an independent diagnostic indicator for OP. However, it has some advantages in reflecting bone marrow conversion as well as microstructural changes in bone trabeculae, during the development of OP, and can be used as a complement to FF and BMD for fine quantitative assessment of OP.

There were still some deficiencies in this study. First, this study was performed at a single center on a small number of subjects. Studies including larger patient cohorts in multicentric trials will be necessary to further demonstrate the robustness of IDEAL-IQ results. Second, due to software reasons, we did not guarantee that the shape and area of the ROIs were consistent, although they were carefully placed in the first 2/3 of the cancellous bone of the vertebral body, which might also have caused some potential errors.

In conclusion, R2* based on IDEAL-IQ sequences has a definite linear relationship with FF and BMD, but it is not yet sufficient as a separate clinical diagnostic indicator and can be used as a complement to FF and BMD for quantitative assessment of OP.

Acknowledgements At the point of finishing this paper, I'd like to express my sincere gratitude to all my colleagues in the Department of Spine Surgery and Radiology, who were of great assistance in the screening and scanning of cases for the completion of this study.

Funding This work was supported by Shaanxi Provincial Key R & D Plans (2021SF-240) and Shaanxi Provincial Key Research and Development Program (2020GXLH-Y-027). The funders had no role in study design, data collection and analysis, decision to publish, or preparation of the manuscript.

Declarations

Guarantor The scientific guarantor of this publication is Prof. Yonghong Jiang.

Conflict of interest The authors declare that they have no conflict of interest.

Statistics and biometry No complex statistical methods were necessary for this paper.

Informed consent Written informed consent was obtained from all patients.

Ethical approval The study was approved by the ethics committee of Honghui Hospital Affiliated Xi'an Jiaotong University (IRB No. 201902068)

Methodology
- prospective
- diagnostic or prognostic study
- performed at one institution

References

1. Haseltine KN, Chukir T, Smith PJ, Jacob JT, Bilezikian JP, Farooki A (2021) Bone mineral density: clinical relevance and quantitative assessment. J Nucl Med. 62(4):446–54
2. Morse LR, Biering-Soerensen F, Carbone LD et al (2019) Bone mineral density testing in spinal cord injury: 2019 ISCD official position. J Clin Densitom 22(4):554–66
3. de Araujo IM, Parreiras ESLT, Carvalho AL, Elias J Jr, Salmon CEG, de Paula FJA (2020) Insulin resistance negatively affects bone quality not quantity: the relationship between bone and adipose tissue. Osteoporos Int 31(6):1125–33
4. Zhang Y, Zhang C, Wang J, Liu H, Wang M (2021) Bone-adipose tissue crosstalk: role of adipose tissue derived extracellular vesicles in bone diseases. J Cell Physiol 236(11):7874–86
5. Veldhuis-Vlug AG, Rosen CJ (2018) Clinical implications of bone marrow adiposity. J Intern Med 283(2):121–39
6. Cheng X, Blake GM, Guo Z et al (2019) Correction of QCT vBMD using MRI measurements of marrow adipose tissue. Bone 120:504–11
7. Bredella M, Daley S, Kalra M, Brown J, Miller K, Torriani M (2015) Marrow adipose tissue quantification of the lumbar spine by using dual-energy CT and single-voxel (1)H MR spectroscopy: a feasibility study. Radiology 277(1):230–5
8. Chiarilli MG, Delli Pizzi A, Mastrodicasa D et al (2021) Bone marrow magnetic resonance imaging: physiologic and pathologic findings that radiologist should know. Radiol Med 126(2):264–76
9. Karampinos DC, Ruschke S, Dieckmeyer M et al (2018) Quantitative MRI and spectroscopy of bone marrow. J Magn Reson Imaging 47(2):332–53
10. Aoki T, Yamaguchi S, Kinoshita S, Hayashida Y, Korogi Y (2016) Quantification of bone marrow fat content using iterative decomposition of water and fat with echo asymmetry and least-squares estimation (IDEAL): reproducibility, site variation and correlation with age and menopause. Br J Radiol 89(1065):20150538
11. Jeon K, Lee C, Choi Y, Han S (2021) Assessment of bone marrow fat fractions in the mandibular condyle head using the iterative decomposition of water and fat with echo asymmetry and least-squares estimation (IDEAL-IQ) method. PLoS One 16(2):e0246596
12. Ergen F, Gulal G, Yildiz A, Celik A, Karakaya J, Aydingoz U (2014) Fat fraction estimation of the vertebrae in females using the T2*-IDEAL technique in detection of reduced bone mineralization level: comparison with bone mineral densitometry. J Comput Assist Tomogr 38(2):320–4
13. Ji Y, Hong W, Liu M, Liang Y, Deng Y, Ma L (2020) Intervertebral disc degeneration associated with vertebral marrow fat, assessed using quantitative magnetic resonance imaging. Skeletal Radiol 49(11):1753–63
14. Sollmann N, Becherucci EA, Boehm C et al (2021) Texture analysis using CT and chemical shift encoding-based water-fat MRI

can improve differentiation between patients with and without osteoporotic vertebral fractures. Front Endocrinol 12:778537
15. Leonhardt Y, Gassert FT, Feuerriegel G et al (2021) Vertebral bone marrow T2* mapping using chemical shift encoding-based water-fat separation in the quantitative analysis of lumbar osteoporosis and osteoporotic fractures. Quant Imaging Med Surg. 11(8):3715–25
16. Schmeel FC, Luetkens JA, Feisst A et al (2018) Quantitative evaluation of T2* relaxation times for the differentiation of acute benign and malignant vertebral body fractures. Eur J Radiol. 108:59–65
17. Zeng Z, Ma X, Guo Y, Ye B, Xu M, Wang W (2021) Quantifying bone marrow fat fraction and iron by mri for distinguishing aplastic anemia from myelodysplastic syndromes. J Magn Reson Imaging. 54(6):1754–1760
18. Shan B, Ding H, Lin Q, et al (2022) Repeatability and image quality of IDEAL-IQ in human lumbar vertebrae for fat and iron quantification across acquisition parameters. Comput Math Methods Me. https://doi.org/10.1155/2022/2229160
19. Wehrli FW, Song HK, Saha PK, Wright AC (2006) Quantitative MRI for the assessment of bone structure and function. NMR Biomed. 19(7):731–64
20. Liau J, Shiehmorteza M, Girard OM, Sirlin CB, Bydder M (2013) Evaluation of MRI fat fraction in the liver and spine pre and post SPIO infusion. Magn Reson Imaging. 31(6):1012–6
21. Watanabe D, Kimura T, Yanagida K et al (2022) Feasibility of assessing male osteoporosis using MRI IDEAL-IQ sequence of proximal femur in prostate cancer patients. Aging Male. 25(1):228–33
22. Ward RJ, Roberts CC, Bencardino JT et al (2017) ACR Appropriateness criteria osteoporosis and bone mineral density. J Am Coll Radiol 14(5S):S189–S202
23. Sebo Z, Rendina-Ruedy E, Ables G et al (2019) Bone marrow adiposity: basic and clinical implications. Endocr Rev 40(5):1187–206
24. Pino AM, Miranda M, Figueroa C, Rodriguez JP, Rosen CJ (2016) Qualitative aspects of bone marrow adiposity in osteoporosis. Front Endocrinol 7:139
25. Singhal V, Bredella MA (2019) Marrow adipose tissue imaging in humans. Bone 118:69–76
26. Tratwal J, Labella R, Bravenboer N, et al (2020) Reporting guidelines, review of methodological standards, and challenges toward harmonization in bone marrow adiposity research. Report of the methodologies working group of the International Bone Marrow Adiposity Society. Front Endocrinol. 11:65